18th Australasian Fluid Mechanics Conference
Launceston, Australia
3-7 December 2012

Numerical Investigation of Performance of a New Type of Savonius Turbine

A. Al-Faruk[1], S.A. Sharifian[1] and S. Al-Atresh[1]

[1]Computational Engineering and Science research Centre (CESRC), Faculty of Engineering and Surveying, University of Southern Queensland, Toowoomba, Queensland 4350, Australia

Abstract

Wind energy is non-polluting and is freely available in many areas and is gaining popularity among researchers. Among wind turbines, Horizontal Axis Wind Turbines (HAWT) are more common compared to Vertical Axis Wind Turbines (VAWT) mainly because of their higher efficiency. However, Savonius turbine of VAWT type has many advantages over others such as simplicity in construction, lower cost of production, constancy of the output power regardless of the wind direction, and good starting torque at low wind speed. It is conceived that the efficiency of the Savonius turbines can be increased using industrial wasted heat primarily due to their structural similarity with the split chambers which are often used to induce fire-whirls in laboratories. This work deals with a basic design of such combined configuration and compares its efficiency with a conventional Savonius turbine. The computational results show that the new design has a higher steady state angular velocity as well as higher coefficient of power than the conventional Savonius turbine.

Introduction

Global warming is the greatest threat facing our planet and continues to be a subject of intense public and political debate. Humans are causing global warming by adding huge amounts of carbon dioxide (CO_2) and other greenhouse gases to the atmosphere. The main source of greenhouse gases is burning fossil fuels for energy production. It is necessary to develop renewable energy and improve energy efficiency of existing systems to reduce greenhouse gas emissions. Wind energy is one of the most promising sources of renewable energy. It is pollution-free, abundantly available in the earth's atmosphere, can be locally converted, and can thus help in reducing our reliance on fossil fuels. Many developed and developing countries have realized the importance of wind as an important resource for power generation and necessary measures are being taken up across the globe to tap this energy for its effective utilization in power production.

Wind turbines are classified based on the axis of rotation of the blades. Horizontal Axis Wind Turbines (HAWTs) are more common compared with Vertical Axis Wind Turbines (VAWTs) mainly because they have higher efficiency. Significant research and investments made for HAWTs have overshadowed progress in VAWTs technology. However, VAWTs have several advantages and promise even higher reliability than HAWTs. A vertical axis wind machine proposed by Finnish Engineer Sigurd Savonius [11] is basically a drag type rotor. However, it generates power through the combined effect of drags and the lift forces [1]. The concept of the conventional Savonius rotor is based on cutting a cylinder into two halves along the central plane and then moving the two half cylinders sideways along the cutting plane, so that the cross-section resembles the letter S shown in figure 1(a). There is some re-circulation of airflow between two blades of the rotor. Air strikes one blade and then is directed to the gap between the two blades and finally to the second blade. A review of Savonius rotor advantages and disadvantages is presented in Menet [8]. The simple structure Savonius rotors are easy to build and their maintenance is very simple. The compact, low cost rotor has the ability to accept wind from any direction thus does not need orientation mechanism which gives high reliability. The efficiency does not decrease significantly when it is exposed to turbulence, gusting and change of wind direction. The components of the vertical turbines can be placed at the ground and their output is steadier than that of HAWTs. Their high starting torque enables them not only to run, but also to start whatever the wind velocity. The high starting torque characteristic have made the Savonius rotor popular for ventilations and pumping applications. They have also been used as start-up device for Darrieus rotors and for small scale power generation. However their slow running behaviour (the blades are running at a speed of the same order as the wind velocity e.g., tip speed ratio $\gamma \approx 1$), and low power coefficient ($C_p \approx 0.15$) compared with HAWTs and Darrieus wind turbines makes them inefficient to be used in a large scale renewable energy project.

In this work, an innovative low cost technique is considered to increases the low efficiency of the conventional Savonius turbines [6,8] using industrial waste heat or natural heat sources. Waste heat or low-grade heat refers to heat produced during industrial processes such as power plants, steel or glass making plants, air conditioning systems and vehicle exhausts and have no useful application due to the associated cost and possible adverse effects on the efficiency of the primary system. Low temperature heat contains very little capacity to do work and rejected to the environment. A system that is not expensive and does not degrade the efficiency of the main system is desirable. It was perceived that a simple and an inexpensive configuration exists which produces a swirling flow and might be able to simultaneously resolve issues associated with cost and efficiency.

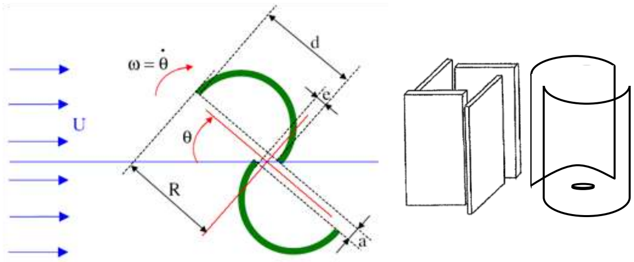

(a) (b)

Figure 1. (a) Schematic of Savonius rotor (adapted from Menet [9]); (b) Two common stationary enclosures to induce fire-whirl: "square enclosure (left) and cylindrical enclosure (right)".

Fire whirls are rare natural phenomena, but potentially catastrophic form of fire. Two fundamental conditions that should exist to generate a fire-whirl are a heat source and a source of angular momentum. Fire-whirls can be induced naturally as well as experimentally. There are currently several configurations to produce fire-whirls in laboratories. The enclosure with a specific pattern directs surrounding air towards the rising gas in a manner that produces circulation. The two common stationary configurations that induce fire whirls are square enclosure as in Satoh and Yang [10] and cylindrical enclosure found in Hassan et al. [5] as shown in figure 1(b).

The obvious geometric similarities between the cylindrical enclosure to induce the fire-whirl and the Savonius turbine make it possible to combine the two mechanisms into one. The industrial waste heat could replace the fire and the turbine's cylindrical enclosure provides the required angular momentum. This research does not consider the fire-whirl mechanism as a sole technique to produce power instead focus on utilizing it as an auxiliary system in an effort to increase efficiency. To combine the two mechanisms, some modifications to the Savonius turbine would be necessary which results to a new type of Savonius turbine. This study numerically investigates the performance of the combined configuration and compares its performance with the conventional Savonius turbine.

Geometry of the designs

A Savonius turbine has a simple structure. The whole rotor turning around a vertical axis is composed of two vertical half-cylinders, as shown in figure 1(a). The rotor is slow running due to the fact that one bucket moves against wind. Geometries of the conventional Savonius wind rotor used in this study have been taken equal with those in the experimental study of Altan et al. [2]. In the present study, the conventional rotor shown in figure 2 has been modelled considering 2 mm thick plate with a nominal diameter (d) of 17.10 cm of height (H) of 32 cm. The optimum overlap ratio (e/d) value has been found as 0.15 by Fujisawa [3], thus the gap distance (e) becomes 2.6 cm and the rotor diameter (D) is calculated as 32 cm. Experiments at an overlap ratio of 0.15 and an aspect ratio (H/D) of 1.0 have been reported to have a maximum power coefficient by Fujisawa and Gotoh [4] and Kamoji et al. [7]. The lower and upper blade end plates of the rotor have been modelled considering plates of 4 mm thickness and diameter (Do) of 35.2 cm which is 10% larger than the rotor diameter [9]. The Savonius wind rotor shaft has been supported near the top and bottom which has a diameter equal to 2 cm. The mass of the rotor is calculated as 3.2132 kg assuming aluminium plates is used to make the rotor.

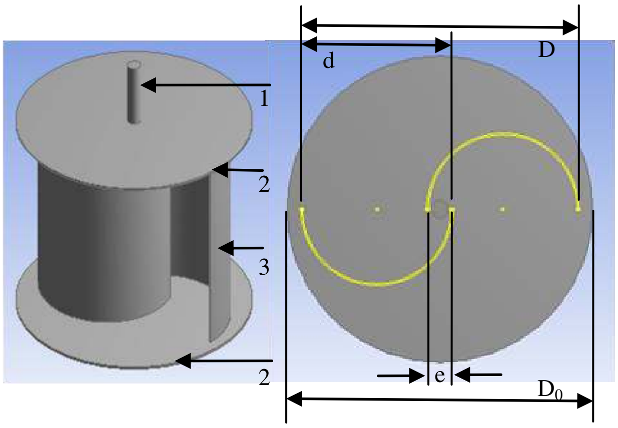

Figure 2. The conventional Savonius wind rotor and its geometrical parameters: 1, Shaft; 2, End plates; and 3, Savonius bucket.

The new rotor also has been modelled considering 2 mm thick plate with the rotor diameter (D) and height (H) of 0.32 cm, the same as that of the conventional one. In both cases, the rotor swept areas are equal which ensures the same amount of input wind energy. In the new design the bucket overlap distance (e) is increased to 8.55 cm to accommodate a circular hole of 4 cm diameter in the centre of the bottom end plate through which the hot air enters the swirling chamber. The bucket inner tips are extended further 30 degree to reduce the air entrainment gap. The nominal diameter (d) of the bucket is calculated to be 20.075 cm and the upper and bottom end plates diameter (D_0) is 35.2 cm the same as the conventional one. However, their thickness has been adjusted to new values in order to keep the rotor weight unchanged (3.2132 kg). In the new rotor, upper shaft diameter is also 2 cm but the lower shaft is split from its middle position to the bottom end plate to allow entrance of the hot air from below (see figure 3).

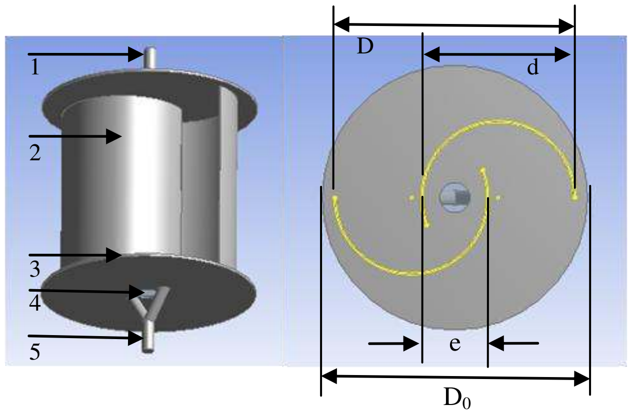

Figure 3. The combined new wind rotor and its geometrical parameters: 1, Shaft; 2, Modified Savonius bucket; 3, End plate; 4, Hot air inlet; and 5, Split bottom shaft

Modelling

Modelling the fluid-structure interaction (FSI) is a problem in many industrial applications and the accuracy of the model and computational cost are heavily influenced by the assumptions made on the nature of the fluid (viscous-inviscid) and on the structure (rigid-deformable). The model treated in this work is a two-way coupling type (reciprocal influences of fluid and solid are modelled); the rotor was treated as a rigid body while the fluid was modelled as incompressible and viscous. The main problem in the fluid-structure interaction modelling is the procedure used to take into account the motion of the solid body in the solution of the fluid-dynamics equations. The strategy to solve this problem used in this work was a Rigid Body Solver with Sliding Mesh Model (SMM) approach.

The rotor was treated as a rigid body which moves due to the fluid forces and torques acting upon it. The rotor is defined in the set up as a collection of two-dimensional regions that form its faces by the surrounded fluid domain. The rotor itself is not a domain, so was not meshed itself. The mass and the absolute values of the mass momentum of inertia for the rotor with respect to a corresponding coordinate system were specified, as well as the gravity force and the external torque (in the case of loaded turbine). The rotor is fixed to the top and bottom shafts and allowed to have a rotational motion about the vertical y-axis. The structural deformations of rotor were neglected but its kinematics was considered; hence the motion of the solid is determined by integrating the second cardinal equation of dynamics for 1-DOF (Degree of Freedom) rotating system which is referred to the fixed rotation axis of the system. Torques acting on the rigid body are the aerodynamic moment and the resistant torque.

The computational fluid domain was divided into two parts. The inner cylindrical domain that contains the rotor and undergoes mesh deformation when the rotor turns, while the outer rectangular domain remains steady, the cylindrical domain was therefore defined as a sub-domain, see figure 4 and 5. To allow mesh deformation, the mesh motion has been defined in the cylinder domain. The mesh motion of the 2D wall boundaries which form the rotor surface followed the rigid body solution. The mesh motion on the wall, symmetry and pressure outlets were set to unspecified. Thus their mesh motion was determined by the motion set on other regions of the mesh. The same setting has been applied to the sub-domain as well. However, to prevent the nodes on the sub-domain interface to move relative to the local boundary frame, the mesh motion of the interface has been set to stationary. Therefore the whole cylindrical sub-domain moved with the same angular velocity as that of the rotor. The interface between the rotating cylindrical domain and stationary rectangular domain was handled by the sliding mesh feature. The fluid-fluid interfaces between the two mesh domains were set to conservative interface flux conditions in order to allow the quantities (mass and momentum, turbulence, and heat transfer) to flow between the current boundary and the boundary on the other side of the interface.

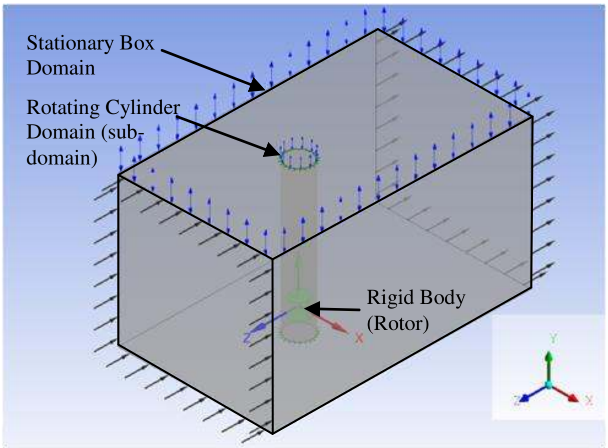

Figure 4. The computational fluid domain consists of a fix box and a rotating cylinder. The cylindrical domain encloses the rotor and can rotate about the y-axis.

A schematic of the computational domain, including the cylinder which represents the rotating portion of the domain, is presented in figure 5. The computational domain extended 2 m upstream, 3 m downstream of the rotor and 1.5 m away from the rotor in the two side walls. The height of the domain is 3 m. All surfaces of the rotor have been defined as no-slip wall boundary condition. The inlet had a uniform velocity of 5 m/s, the outlet had a zero relative static pressure boundary condition, the top had an opening boundary with the zero relative pressure and unknown direction, and the remaining two sides and the ground had a free no slip wall boundary conditions. The size of the computational domain was chosen so that the boundaries would not affect the performance of the turbines. In the case of the new turbine, the hot air inlet is $100\ ^{\circ}\mathrm{C}$ at atmospheric pressure condition. The k-ε turbulence model with 5% turbulence intensity was used for the simulations. The 0.32 m diameter rotor was placed inside the cylindrical rotating region which has a diameter of 0.50 m.

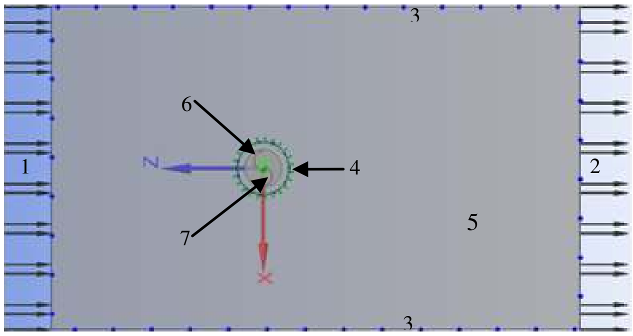

Figure 5. Top view of the computational domain and boundary conditions: 1, Inlet with known velocity; 2, Outlet with known pressure; 3, No-slip side walls; 4, Interface; 5, Stationary rectangular fluid domain; 6, Rotating cylinder domain; and 7, Rotor bucket with no-slip condition.

Results and Discussions

The simulations of the conventional Savonius rotor and combined new rotor has been conducted using the rigid body solver and the sliding mesh approach at a uniform velocity of 5 m/s (Re = 103550) in order to characterize the performance of the new combined rotor and to compare it with the conventional Savonius rotor. The angular velocity and the rotor torque values about the vertical axis (y-axis) with the physical simulation time have been taken from the simulation. These values were used to analyse the performance of the rotors in terms of power coefficient (ratio of mechanical power in the shaft to wind power). The performance parameters of the rotors are discussed in two cases of unloaded and loaded (0.05 Nm in negative direction).

Angular Velocity

The comparison of angular velocities between the conventional Savonius rotor and the new rotor without load and with load (0.05 Nm in the negative direction) conditions are presented in figures 6 and 7, respectively. In unloaded condition, the steady state angular velocity of the new turbine is 27.80 rad/sec which is about 35% higher than that obtained for the conventional turbine (20.6 rad/sec). In the loaded case, the steady state angular velocities are subsequently reduced to 19.0 rad/sec and 10.7 rad/sec respectively for the conventional and the new turbine. It is noticeable from the two figures that the loaded turbines reached steady state values in longer times (at about 150 sec) than the unloaded turbines (at about 100 sec).

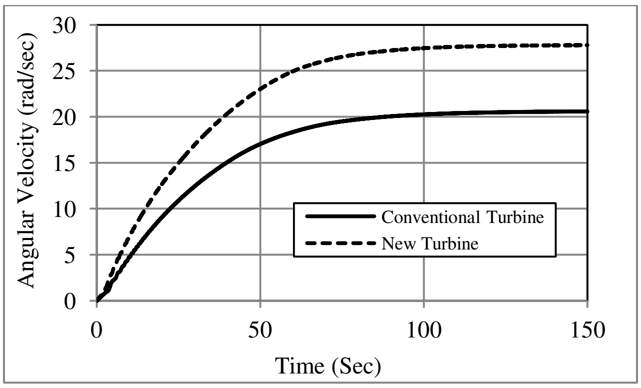

Figure 6. Comparison of angular velocity between the conventional Savonius turbine and the new combined turbine (No load condition)

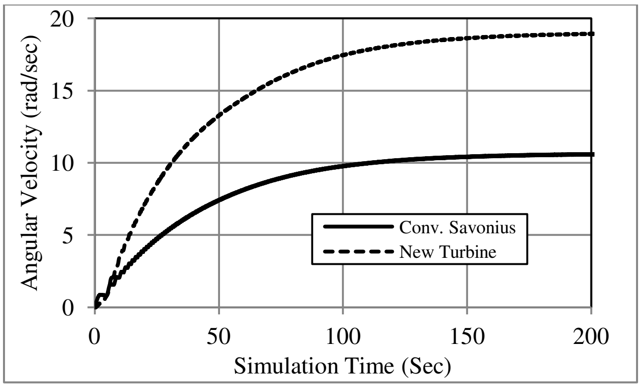

Figure 7. Comparison of angular velocity between the conventional Savonius turbine and the new combined turbine (with load condition)

Coefficient of Power

The variation of the average power coefficient with the tip speed ratio (the ratio of outer tip velocity of the bucket to the wind velocity) for both the unloaded and loaded turbines as shown in figure 8 and 9, respectively. The C_p increases with the increase in tip speed ratio to a maximum value then again decreases to zero for the unloaded case. Figure 8 indicates a maximum C_p of 7% at a tip speed ratio of 0.38 for the conventional turbine and of 13% at a tip speed ratio of 0.52 for the new turbine. When the turbine is loaded, the C_p also increases with tip speed ratio and reaches a maximum value of 25% (at the tip speed ratio of 0.60) and 14% (at the tip speed ratio of 0.35) for the new and conventional turbine, respectively, as shown in "figure 9". It is noticeable that with adding load on the rotor, the angular velocity decreases, but the power coefficient increases.

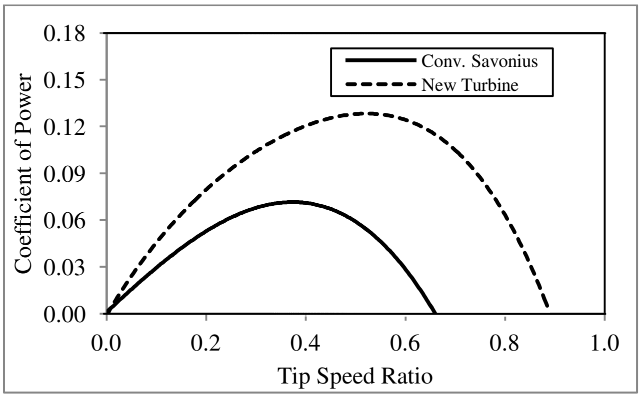

Figure 8. Coefficient of Power *(C_p)* comparison between the conventional Savonius turbine and the new combined turbine (No load condition)

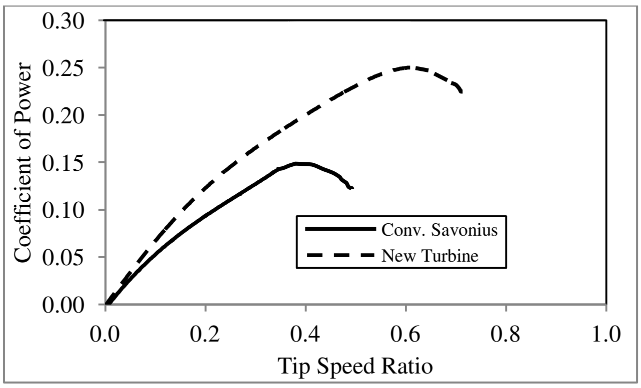

Figure 9. Coefficient of Power *(C_p)* comparison between the conventional Savonius turbine and the new combined turbine (with load condition)

Conclusions

In this study, a numerical study has been carried out in order to improve the performance and increase the power coefficient of Savonius wind turbine incorporating a hot swirling flow inside the turbine enclosure with modified Savonius bucket. Simulations of new designed turbine as well as conventional Savonius turbine in two different load conditions are conducted at a uniform velocity and then their performance are compared. The comparisons show that the new design offers significant improvement in performance. The angular velocity of the new turbine is increased by 35% and 77.5% for the unloaded and the loaded case, respectively. The power coefficient (C_p) of the new turbine is also increased by 85.5% and 78.5% for the unloaded and the loaded case, respectively.

Acknowledgements

The first author expresses his appreciation for the financial support from Australian government through IPRS scholarship.

References

[1] Akwa, J.V., Silva Jr, G.A. & Petry, A.P., Discussion on the verification of the overlap ratio influence on performance coefficients of a Savonius Wind Rotor using Computational Fluid Dynamics, Renewable Energy, 38, 2012, 141-149.

[2] Altan, B.D., Atilgan, M. & Ozdamar, A., An Experimental Study on Improvement of a Savonius Rotor Performance with Curtaining, Experimental Thermal and Fluid Science, 32, 2008, 1673-1678.

[3] Fujisawa, N., On the Torque Mechanism of Savonius Rotors, Journal of Wind Engineering and Industrial Aerodynamics, 40, 1992, 148-152.

[4] Fujisawa, N. & Gotoh, F., Experimental Study on the Aerodynamic Performance of a Savonius Rotor, Journal of Solar Energy Engineering, Transactions of the ASME 116, 1994, 148–52.

[5] Hasan, M.I., Kuwana, K., Saito, K. & Wang, F., Flow Structure of a Fixed-frame type Fire-whirl, 8^{th} International Symposium on Fire Safety Science, USA, 2005.

[6] Kamoji, M.A., Kedare, S.B. & Prabhu, S.V., Performance tests on Helical Savonius Rotors, Renewable Energy, 34, 2009, 521-529.

[7] Kamoji, M.A., Prabhu, S.V. & Kedare, S.B., Experimental Investigations on the Performance of Conventional Savonius Rotor under Static and Dynamic Conditions, 33rd National and 3rd International Conference on Fluid Mechanics and Fluid Power, Research Publishing Services, December 2006.

[8] Menet, J.L., A Double-step Savonius Rotor for Local Production of Electricity: A Design Study, Renewable Energy 29, 2004, 1843-1862.

[9] Menet, J.L. & Bourabaa, N., Increase in the Savonius Rotors Efficiency via a Parametric Investigation.

[10] Satoh, K. & Yang, K.T., Simulations of Swirling Fires Controlled by channeled self-generated entrainment flows, 5^{th} International Symposium on Fire Safety Science, 1997.

[11] Savonius, S.J., The S-rotor and its Applications. Mechanical Engineering, 53(3), 1931, 333-338.